

Some basic relationships between density values in cancellous and cortical bone

Peter Zioupos^{a,*}, Richard B. Cook^b, John R. Hutchinson^c

^a*Biomechanics Laboratories, Department of Materials & Applied Science, Cranfield University, Shrivvenham, UK*

^b*Department of Oral Rehabilitation, School of Dentistry, Otago University, Dunedin, New Zealand*

^c*Structure and Motion Laboratory, The Royal Veterinary College, University of London, Hatfield, UK*

Accepted 28 March 2008

Abstract

Density is a salient property of bone and plays a crucial role in determining the mechanical properties of both its cancellous and cortical structural forms. Density is defined in a number of ways at either the bone tissue (D_{app} , apparent) or the bone material level (D_{mat} , material). The concept of density is relatively simple, but measuring it in the context of bone is a complex issue. The third dimension of the problem is the concept of porosity, or BV/TV (ratio of bone material volume over tissue volume). Recent investigations from our laboratory have revealed an interdependence of D_{app} and D_{mat} in the cancellous bone of at least four different cohorts of human patients. To clarify the underlying causes of this behaviour, we produced here equivalent relationships from specimens originating from cortical and cancellous areas of the same bone. Plots of D_{app} vs. D_{mat} showed that D_{mat} was not a monotonic function of increasing D_{app} , but instead showed a ‘boomerang’-like pattern. By empirically dissecting the data in two regions for D_{app} above and below a value equal to 1.3 g cm^{-3} , we were able to objectively isolate the bone in trabecular and compact forms. Our findings may have implications not only for the segregation of bone in these two structural forms, but also for the mechanobiological and physiological processes that govern the regulation of compact and trabecular bone areas.

© 2008 Elsevier Ltd. All rights reserved.

Keywords: Bone; Cancellous; Cortical; Density; Porosity; BV/TV; Mineral content

1. Introduction

Density is a salient property of bone and plays a crucial role with respect to its mechanical properties in both its cancellous and cortical structural forms. Density is defined in a number of ways at either the bone tissue or the bone material level. Customarily the wet mineralised mass of bone at the tissue level over the volume occupied by the tissue defines the ‘apparent’ density value. The same mass of bone material over the volume occupied by the material itself defines the ‘real’ or ‘material density’ of bone. The difference between the two of course is due to the presence of pores or the vacuous spaces that are related to the

canaliculi, osteocyte lacunae, osteonal canals and analogous non-mineralised architectural features.

The concept of density is relatively simple, but measuring it in the context of bone is a complex issue. Studies have argued that particular attention must be paid to the flushing of the liquid from the pores and then re-filling them with the suspending fluid when applying Archimedes’ principle (Aspden and Li, 1998). Others commented that defatting and/or preserving the marrow may have an effect if it interferes with the re(de)hydration process (Sharp et al., 1990). Subsequent studies reported substantial differences in density values obtained by the invasive/in-vitro Archimedes’ principle and the non-invasive DXA or microCT methods (Keenan et al., 1997).

The third dimension in the problem is the concept of porosity, or its recently popular surrogate BV/TV (ratio of bone material volume over tissue volume). This has gained prominence probably due to the simplicity of the concept.

*Corresponding author. Tel.: +44 1793 785932; fax: +44 1793 783076.

E-mail addresses: p.zioupos@cranfield.ac.uk (P. Zioupos), richard.cook@dent.otago.ac.nz (R.B. Cook), jrhhutch@rvc.ac.uk (J.R. Hutchinson).

The ratio of volumes represents a geometric and visible marker of the level of porosity in the structure. The value of BV/TV is however, relative to the value of D_{app} and D_{mat} . For suitably altered apparent density vs. material density values, two obviously different cancellous structures can have the same nominal BV/TV.

D_{app} is a primary influence of mechanical properties (Rice et al., 1988) at the tissue/structural level, while D_{mat} determines material behaviour at the trabecular level and later, by implication, properties at the structural level. BV/TV features prominently in experimental studies of cancellous bone mechanics, but also indirectly, in theoretical studies as it relates linearly to the ratio of D_{app}/D_{mat} , which is the normalised density of the structure (example in Fig. 1) as used in the models by Gibson and Ashby (1997). In FEA applications, the structure is often obtained from CT scans and directly downloaded into the computer and meshed into a FE model. Material properties for the voxels are derived from the relative radio-density in Hounsfield units (HU). It is unclear, however, what essence of bone substance these scans capture. Are HU more closely correlated to density variables, or to BV/TV?

Overall there have been only a handful of papers that deal with density measurements per se, and to the best of our knowledge no article has paid particular attention to the relationships between the three aforementioned quantities (D_{app} , D_{mat} , BV/TV). Our previous studies have revealed an interdependence of D_{app} – D_{mat} in at least four different cohorts of patients who underwent surgery following either osteoporotic or osteoarthritis complications (Zioupos and Aspden, 2000; Coats et al., 2003;

Zioupos et al., 2008). As shown in Fig. 2, plots of apparent to material density show strong negative correlations. Increases in apparent density were accompanied with associated decreases in material density of the trabeculae. This in itself constitutes a paradox as hypothetically the limit of apparent density ought to be the actual material density of the tissue. In other words, for a typical material bone matrix density of 2.2 g cm^{-3} (roughly the grand average of all values quoted in the literature), the end point of the process of gradually reducing pore sizes, and thus increasing apparent density, should also be 2.2 g cm^{-3} (Fig. 2). A small number of data points from osteoarthritic (OA) material showed such a trend, but it is uncertain whether this is due to the abnormalities observed in OA matrix, which shows proliferation of osteoid tissue and compact-like bone areas.

We were not able to find similar reference to an inverse D_{app} – D_{mat} relationship anywhere in the literature, but we identified at least three independent studies, where the progress of material trabecular density showed an inverse effect to the structural mechanical integrity of cancellous bone itself (Galante et al., 1970; Nicholson et al., 1997; McNamara et al., 2005), thus corroborating indirectly our original observations. We are uncertain on the likely causes of this behaviour and we hypothesised that the effects are either specific to the structural form of bone (cortical vs. cancellous), or specific to the condition associated with the nature of the tissue (OP/OA/healthy donors, Coats et al., 2003), or these may be due to inter-individual vs. intra-individual effects (Zioupos et al., 2008). Such questions can only be elucidated by producing equivalent relationships

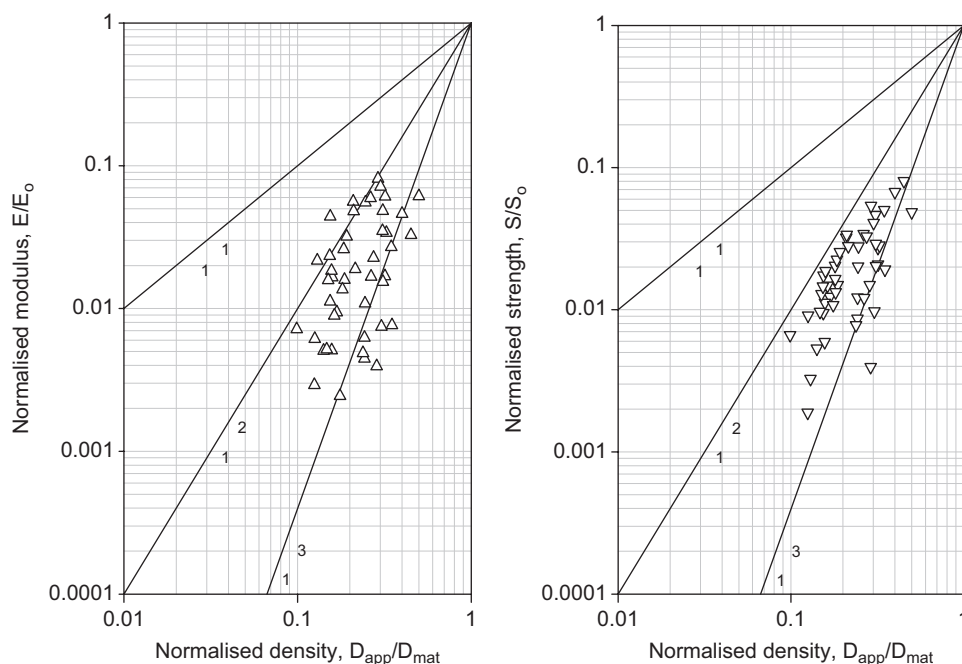


Fig. 1. Normalised plots (as per Gibson and Ashby, 1997) for elastic modulus and strength vs. density for femoral head cancellous bone cores aligned along the predominant trabecular direction for a group of 30 victims of femoral neck fractures (Cook, 2005). For normalisation, the modulus and strength of bone matrix were taken to be $E_0 = 18 \text{ GPa}$, $S_0 = 190 \text{ MPa}$. Normalised density is the actual ratio $D_{app}/D_{mat} = (\text{apparent density}/\text{trabecular material density})$ as measured for each specimen. Lines for the power law relationships of 1, 2 and 3 are also shown.

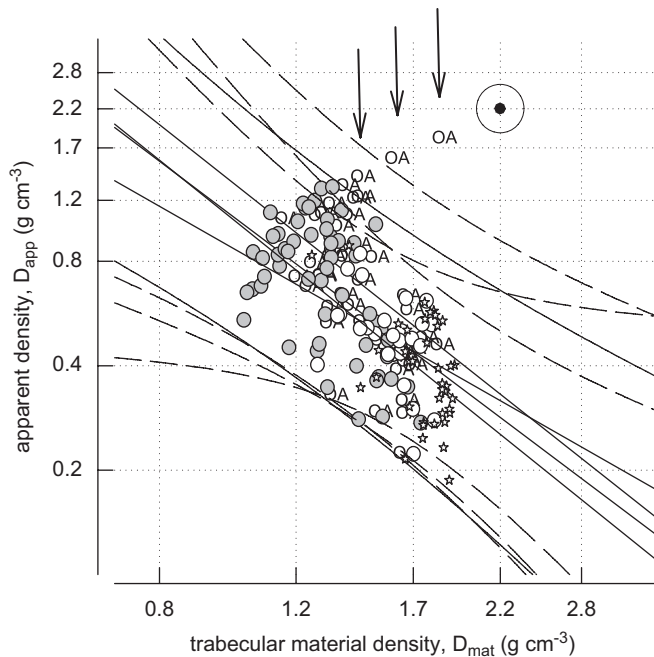


Fig. 2. Apparent (D_{app}) vs. material density (D_{mat}) in four different cohorts (175 samples, 66 OP, 12 OA) of donors (Zioupos and Aspden, 2000; Zioupos et al., 2008) with least squares regressions and the 95% prediction intervals for the data. It is clear that, apart from a small number of OA data (arrows), the general trend does not aim for the customarily assumed hypothetical end-point of the process (encircled) at a nominal bone matrix density of 2.2 g cm^{-3} .

from specimens originating from one and the same healthy bone to remove these confounding factors. This is the aim of the present study.

2. Materials and methods

To achieve this primary aim, we used an animal model, the femur of an elephant (Supplementary e-material #1). This had certain advantages as it is mammalian with the shape and properties at the bone matrix level (confirmed by nanoindentation tests in our laboratories) similar to those of a human femur, the only major difference, therefore, being one of size. Its large size and extensive volumes of cortical and cancellous bone allowed structural effects similar to human tissue to be observed on a scale in tens of millimetres and also allowed us to (1) obtain a large number of specimens; (2) produce all cortical and cancellous samples from the same sections throughout the same bone (no intra- or inter-individual variability), and (3) obtain a sample from an animal known to have previously been healthy. The specimen was the right femur of an adult Asian elephant (3432 kg; 24 years old) and was representative of other elephant femora we have examined recently (Hutchinson et al., 2008). The specimen was collected shortly after the animal's euthanasia (for reasons unrelated to this study) at Whipsnade Zoo (Bedfordshire, UK) and frozen (-20°C) until sample testing.

2.1. Preparation

Two sample designs were prepared. Cortical ($n = 20$) and cancellous ($n = 21$) bone cores were produced using a 9 mm internal diameter core drill with a wafer abrasive particles-impregnated edge. Cores were roughly 18 mm long, so as to produce a length to diameter ratio of 2:1, and were suitable to produce standard biomechanical data (modulus of elasticity, stress at yield, Poisson's ratio values). The cortical cores were removed

mainly from the shaft of the femur at distances of 30, 41, 49, 58 and 71 cm in the distal direction (total length of the femur was 95 cm, roughly twice that of a human) and cores were pointing in the longitudinal direction, so as to align with the haversian/fibrolamellar structure of the tissue. Cancellous cores were prepared mostly from the femoral neck, the head of the femur (normal to the surface) and the cross-sectional slices, where the presence of cancellous bone was evident. For cancellous bone in particular, a larger number of cube-like samples ($10 \times 10 \times 10 \text{ mm}^3$, suitable for measuring anisotropic properties in three principal axes) were also taken from a number of cancellous sites along the length of the whole femur. The cubes were manufactured so that they were aligned not necessarily with the anatomical direction, but with the orientation of the predominant visible trabecular structure. A total of 112 cubes were prepared, with a D_{app} range of $0.283\text{--}1.8 \text{ g cm}^{-3}$.

Each sample was cleaned using a high-pressure water jet to remove any bone marrow and fat, and then left for 48 h in a solution of 1:1 chloroform/ethanol to dissolve any remaining fat. After 48 h, the cubes were rehydrated gradually and washed with water/ethanol mixtures. They were then left to rehydrate fully for a further 24 h in Ringers solution. The dimensions of each specimen were measured using a Vernier callipers to produce a volume measure (V_0). Weights were measured by use of an electronic microbalance (METTER TOLEDO[®] College B154) either in air (W_{weight}) or in submersion (W_{sub}) using a liquid of known density (distilled water, density $\sim 1 \text{ g/cm}^3$). In practice the samples were first degassed thoroughly, then their submerged weight was measured, and then they were weighed in air. This was found to be the most reliable method for measuring W_{sub} and W_{weight} that produced small variability in the results. Before the W_{weight} was taken, samples were placed in a centrifuge (MSE[®] Mistral 1000) for 3 min with a speed of 3000 rev/s to remove excess amounts of water from their major pores. From these values (where ρ is the density of the water solution used) we calculated

$$\text{Apparent density, } D_{app} = W_{weight}/V_0 \quad (1)$$

$$\text{Trabecular material density, } D_{mat} = \rho W_{weight}/(W_{weight} - W_{sub}) \quad (2)$$

$$\text{Porosity (\%), } P = 100[1 - (D_{app}/D_{mat})] \quad (3)$$

$$\text{BV/TV} = D_{app}/D_{mat} \quad (4)$$

2.2. Mechanical testing

The core samples were held in grips (one of which had a 3D articulation) with a miniature contact extensometer attached to them at a central 6 mm gauge. They were constantly irrigated with Ringer's solution at 37°C , were preconditioned for a few cycles to a max strain of 0.1% and, lastly, were taken to just beyond the macroscopic yield to determine Young's modulus and stress at yield and failure values. A further 112 non-destructive tests were performed on the cube-like specimens between two polished loading platens contained within a Ringer's bath system set up to maintain physiological conditions throughout testing. These tests allowed measurements along three orthogonal axes (to observe the degree of anisotropy) and used an external extensometer (they were, therefore, corrected for machine compliance as per the earlier testing methods in the literature; Mitton et al., 1997).

After mechanical testing, a smaller section was removed from each sample, weighed in its hydrated and dehydrated state, then ashed at 600°C for 12 h before being weighed for a third time. The result enabled the determination of the water (Wat%), mineral (Min%) and organic (Org%) content fractions of each individual sample over its initial wet weight.

3. Results

Fig. 3 shows the behaviour of D_{app} vs. D_{mat} for all 153 samples collected from the one elephant femur. The data

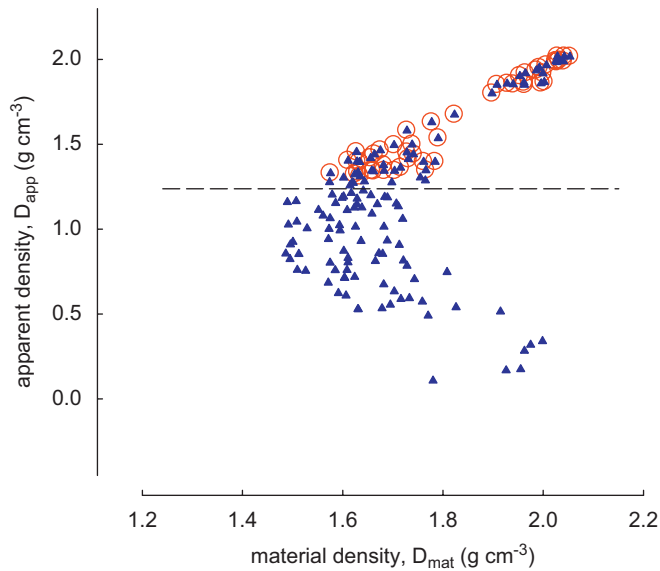


Fig. 3. Apparent (D_{app}) vs. material density (D_{mat}) for all samples (triangles) produced from the same femur in both cortical and cancellous regions. The samples having $D_{app} > 1.3$ are encircled and the same notation is used in the following figures to allow visual comparisons to be made.

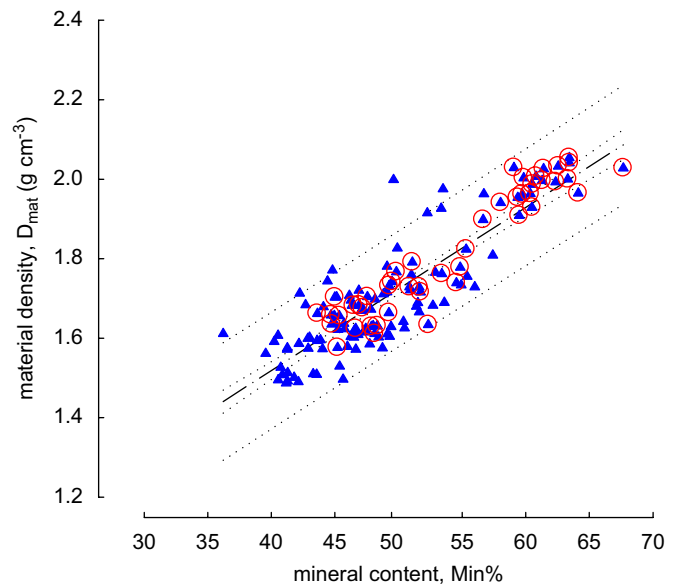


Fig. 4. D_{mat} vs. mineral content (ash weight over wet mineralised weight) for all samples (solid triangles) and those with $D_{app} > 1.3$ (encircled). Least squares linear regression with its 95% confidence interval and the 95% prediction interval for the data; $D_{mat} = 0.70 + 0.02 \times \text{Min}\%$; $R^2 = 0.77$.

show a ‘boomerang’-like pattern with an inflection point at about $D_{app} \sim 1.3 \text{ g cm}^{-3}$ and $D_{mat} \sim 1.60 \text{ g cm}^{-3}$. The horizontal line we have drawn in Fig. 3 was an eyeball estimate to separate the data into two regimes. Samples with D_{app} above 1.3 g cm^{-3} show a positive correlation between the densities; those below show an inverse relationship. Qualitative inspection of the samples above and below the threshold showed that they were indeed coming from cortical areas (or areas consisting of compact bone) and cancellous areas, respectively.

Starting from a point of minimum porosity (intracortical value), D_{mat} appears to reduce to a value of 1.5 g cm^{-3} and then reverses order towards higher values for the most porous of structures. The latter falls in line with our previous studies (Zioupos and Aspden, 2000; Zioupos et al., 2008), which were exclusively on human cancellous bone.

This bimodal behaviour holds only for densities, because as Fig. 4 shows the material density of bone can be explained simply by an increase in the mineral content. The two datasets (for trabecular and compact bone) can be described by one relationship; they overlap remarkably over the full range of D_{mat} , and at least in this respect there is no further conundrum that needs answering.

4. Discussion

We have inspected the basic relationships between density values in cortical and cancellous bone regions in the same bone. We make the note that pores in our analysis cover the full range of shapes and possible values. They are simply the vacuous spaces present in cancellous and compact bone. In cancellous bone they resemble open

spaces and bubble-like cavities. In compact bone the largest component of intracortical porosity is unidirectional and relates to the vascular spaces in the centre of osteons. However, the geometry in itself is not sufficient to produce the effect we see here, the effect related to the physiology of building bone around these spaces. There are two caveats linked to our results. (i) The effect we report is real and not an experimental artefact. For this we have made repeated measurements, by different experimenters, on different cohorts and also verified the basic relationships in two different labs. We can, therefore, vouch that these methods produce this said behaviour at all times. (ii) The bone specimen we used was mammalian. For this, however, in microhardness (60–80 Vickers) and nanohardness (indentation modulus of 17–21 GPa) measurements of the bone matrix, we established that it resembles closely human bone in both substance and form. With these two caveats in mind, we outline the implications of the present findings along three threads.

4.1. Where does cancellous bone start and where does it end?

Until now the quantitative segregation of bone in compact and cancellous forms has not been well defined. Qualitatively and by histological means, one may produce an informed judgment of what is cancellous and what is cortical/compact bone. The evidence, however, is either unsupported and/or it is not numerically explicit. Table 1 summarises succinctly quotes from various researchers spanning more than a century in attempting to define the range of cortical and cancellous bone.

The various anecdotal quotations and figures agree closely with our values. However, our data offers for the

Table 1
Summary of quotes on the range and delineation between cortical/compact and cancellous bone

Reference	Quote	Comment
Wolf (1892)	'... compact bone is simply more dense cancellous bone.'	Personal opinion?
Carter and Hayes (1977)	'... the classification of bone tissue as compact or trabecular is based on bone porosity, which is the proportion of the volume occupied by non-mineralised tissue. Compact bone has a porosity of approximately 5–30%; trabecular-bone porosity may range from approximately 30% to more than 90%. ... However, the distinction between very porous compact bone and very dense trabecular bone is somewhat arbitrary.'	Expressing a generally perceived view arrived at by visual qualitative inspection?
Gibson (1985)	'... bone with a volume fraction of solid less than 70% is classified as cancellous, that over 70% compact.'	-''-
Ashman and Rho (1988)	'... specifically, the density of the structure of cancellous bone previously referred to as apparent density by Carter and Hayes (1977) and as bulk density (Martens et al., 1983), varies from approximately 100–1000 kg m ⁻³ .'	Carter and Hayes (1977); Martens et al. (1983)
Schaffler and Burr (1988)	Indirectly referred: ... to compact bone as having porosity less than approximately 15% and that trabecular bone has a porosity greater than approximately 70%.	A generally perceived view?
Bonucci (2000)	'... the real difference between compact and spongy bone depends on its porosity: that of compact bone, mainly due to the voids provided by osteonal canals, Volkmann's canals, osteocytes and their canaliculi, and resorption lacunae, varies from 5% to 30% (apparent density about 1.8 g cm ⁻³); the porosity of cancellous bone, chiefly due to the wide vascular and bone marrow intertrabecular spaces, ranges from 30% to more than 90% (apparent density 0.1–0.9 g cm ⁻³).'	-''-
Gibson (2005)	'... (cancellous bone) has a cellular structure, with a relative density typically about 0.05 and 0.3.'	-''-

first time, an independent quantitative and unequivocal delineation between cancellous and cortical bone. As shown in Fig. 3, the relationship between D_{app} – D_{mat} shows

an inflection point at about $D_{app} = 1.3 \text{ g cm}^{-3}$ and at $BV/TV = 0.70$. Values of D_{app} and BV/TV above this threshold belong to compact bone areas; values below are in cancellous bone tissue.

4.2. Implications for QCT and D_{app}/D_{mat}

In the light of the present data, one is justified to question what it is that quantitative computer tomography (QCT) and absorptiometry methods actually capture in the scanning of bone tissue. Fig. 4 shows that mineral content has a single linear relationship to the material density (D_{mat}) for both cancellous and compact bone areas, with a significant overlap throughout the range. However, Fig. 3 also shows that D_{mat} behaviour is not monotonic with respect to D_{app} , but it decreases or increases depending on whether the bone area in question is in cancellous or in compact bone tissue.

The main modern use of QCT is the extrapolation of material properties from HU values. Fig. 5 shows elastic modulus values produced here vs. D_{app} , D_{mat} and BV/TV . It is interesting to note that E increases as a high power (or even exponentially) vs. all these three variables. The power exponent gets progressively higher in the order of D_{mat} , D_{app} , BV/TV .

In the case of D_{mat} (Fig. 5b) there is a significant overlap between values for compact and cancellous areas. There is a greater scatter, and if accurate elastic modulus (E) values are required those values would depend on whether the scanned volume was in fact compact or cancellous tissue. For $D_{app} < 1.3 \text{ g cm}^{-3}$, the E value is practically indeterminate by D_{mat} alone and has more to do with the structural effects in cancellous bone. For $D_{app} > 1.3 \text{ g cm}^{-3}$, E is a high power of D_{mat} . By implication if the scanned voxel is very small (in the tens of microns) the assigned E value cannot come from macromechanical relationships like the ones usually employed in recent voxel-based FEA papers (see Schileo et al. (2007), for a review and an assessment of three commonly used functions). If the voxel is small, the E values must come from associations to the mineral content and nano-indentation measurements.

On the other hand, it is encouraging that for D_{app} and BV/TV there is no overlap between E and values for compact and cancellous areas (Fig. 5a and c). Therefore, when scanning of bone tissue volumes on the millimetre scale (which represents mesostructural properties for E , D_{app} , BV/TV), the material can be modelled by adopting E values produced by conventional macromechanical testing like the tests we carried out here. Subsequently, E values can be allocated via a single, albeit high-power law, relationship of E vs. D_{app} , or BV/TV .

In the same context and regarding QCT applications, we must stress that because of the tight relationship between D_{mat} and mineral content (Min%) the relationship between Min% and BV/TV is also bimodal, as shown in Fig. 6. The value for Min% (or its equivalent, the ash content) is

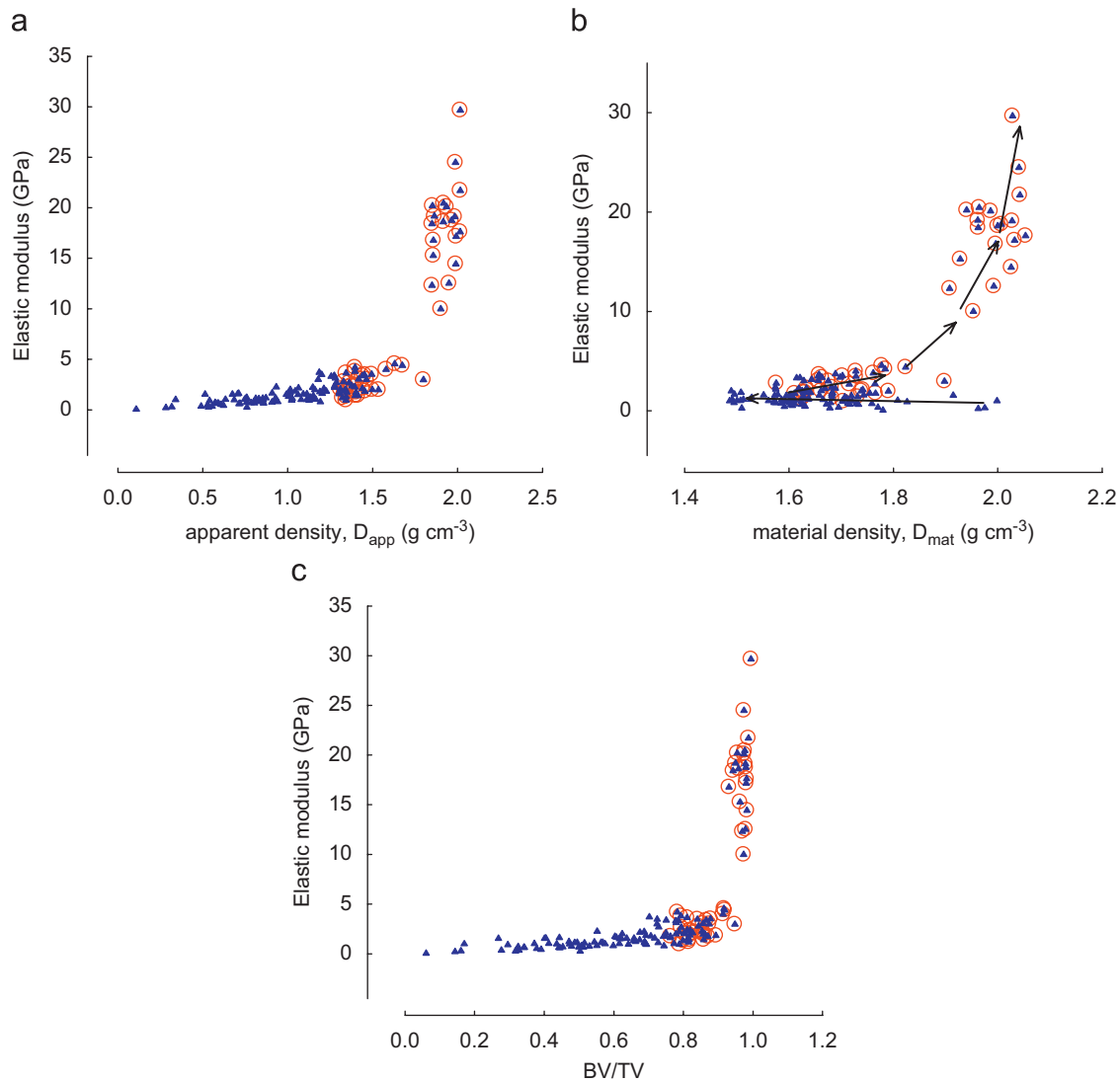


Fig. 5. Plots of E vs. (a) D_{app} , (b) D_{mat} and (c) BV/TV. The arrows in (b) show the trend of data from the lowest to the highest D_{app} values.

occasionally set to be a constant value, or an invariant with the BV/TV. As shown in Fig. 6, this is also not strictly true.

4.3. Bone physiology and mechanobiology

First, it is worth considering the implications of the observed inverse D_{app} – D_{mat} relationship applicable in particular within cancellous bone tissue (Figs. 2 and 3). It has been a long-established belief among biomechanists that the two bone types, cancellous and cortical, express primarily a structural adaptation. In other words, the same substance of cortical bone can be turned into cancellous if one simply increases the pore size. As we pointed out in Fig. 2, this generalisation of a very simple geometric concept is plainly wrong. The line of progress of the two densities would then be aiming towards the point $D_{app}/D_{mat} = 2.2/2.2\ g\ cm^{-3}$. This is not what happens within cancellous bone at least. We can think of two unfolding scenarios to explain this: (i) from biology and a teleological point of view it makes sense, in evolutionary terms, if the

less bone mass there is, the denser the remaining material is to compensate and counteract the detrimental effects on the structure as a whole (assuming of course that bone knows what it is that it is aiming for); or (ii) in terms of chemistry of remodelling action, the behaviour we observe may be simply the result of an increased mineral solubility in areas of lesser density, with the result that denser trabeculae survive as porosity increases precisely because they are denser and more resilient to the osteoclastic activity.

Secondly, our data show that the more porous cancellous structures have denser trabeculae (inverse D_{app} vs. D_{mat} relationship), while more porous compact bone volumes show reduced material density and mineral content (because within compact bone D_{app} and D_{mat} go hand in hand). It appears likely that there are two different tissue physiologies that apply here, or at least there are two different tissue mechanobiology imperatives at play in cancellous and cortical bone, respectively. In cancellous bone, the lower the number of trabeculae that are present,

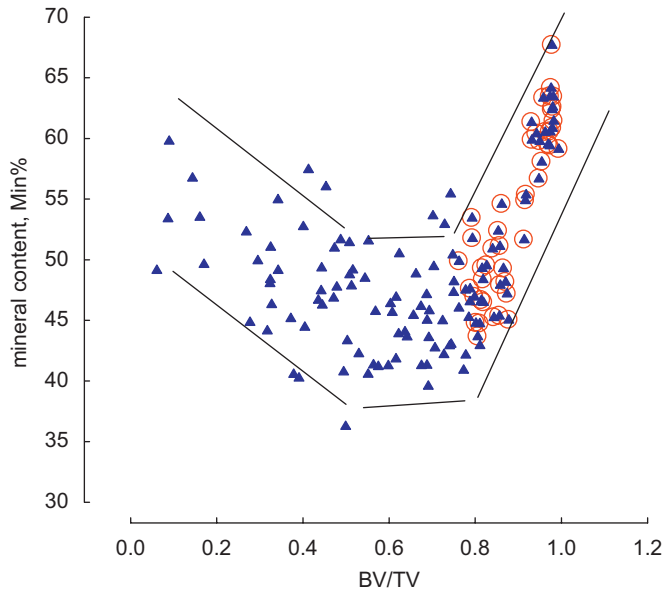


Fig. 6. Mineral content (Min%) vs. BV/TV. The lines denoting the envelope have been drawn by hand.

the denser and stiffer they are. Consequently for the same level of stress, the stiffer material would experience a smaller strain. Smaller strains mean smaller ‘driving signal’ for homeostasis, but also ultimately lesser damage. If that is the ‘imperative’ for cancellous bone, then avoiding damage and resorption (resulting from loss of connectivity) is what drives the process forward. By comparison, this same argument would not hold for cortical bone where the D_{app} vs. D_{mat} relationship is different. In cortical bone, conventional mechanobiology theories suggest that it reacts positively to strain or strain energy density. Strain helps to maintain mass, which in turn results in the tissue experiencing less strain and an overall equilibrium is preserved.

There may be a very simple explanation of how these two basic principles (strain homeostasis and damage) drive two apparently different pathways. At the same time, the process may have nothing to do with mechanobiology, but more to do with bone physiology and design. We do not pretend to understand these; we are at present simply content to mention the various possibilities.

Conflict of interest statement

There is no conflict of interest.

Acknowledgements

The tests were carried out in the Biomechanics laboratories of the Department of Materials & Applied Science of Cranfield University in Shrivenham, UK. PZ acknowledges the support of the EPSRC (GR/N33225; GR/N33102; GR/M59167). JRH thanks the BBSRC (BB/C516844/1) and the Department of Veterinary Basic Sciences (RVC) for

financial support, and Whipsnade Zoo for provision of the specimen.

Appendix A. Supplementary data

Supplementary data associated with this article can be found in the online version at doi:10.1016/j.jbiomech.2008.03.025.

References

- Ashman, R.B., Rho, J.-Y., 1988. Elastic modulus of trabecular bone material. *Journal of Biomechanics* 21, 177–181.
- Aspden, R.M., Li, B., 1998. Reproducibility using Archimedes’ principle in measuring cancellous bone volume by L. Zou, R.D. Bloebaum and K.N. Bachus. *Medical Engineering and Physics* 20, 159–160.
- Bonucci, E., 2000. Mechanical testing of the bone and the bone–implant interface. In: An, Y.H., Draughn, R.A. (Eds.), *Basic Composition and Structure of Bone*. CRC Press, Boca Raton, FL, pp. 3–22.
- Carter, D.R., Hayes, W.C., 1977. The compressive behaviour of bone as a two phase porous structure. *Journal of Bone and Joint Surgery* 59-A, 954–962.
- Coats, A.M., Zioupos, P., Aspden, R.M., 2003. Material properties of subchondral bone from patients with osteoporosis or osteoarthritis by microindentation testing and electron probe microanalysis. *Calcified Tissue International* 73, 66–71.
- Cook, R.B., 2005. Non-invasively assessed skeletal bone status and its relationship to the biomechanical properties and condition of cancellous bone. PhD Thesis, Cranfield University, UK.
- Galante, J., Rostoker, W., Ray, R.D., 1970. Physical properties of trabecular bone. *Calcified Tissue Research* 5, 236–246.
- Gibson, L.J., 1985. The mechanical behaviour of cancellous bone. *Journal of Biomechanics* 18, 317–328.
- Gibson, L.J., 2005. Biomechanics of cellular solids. *Journal of Biomechanics* 38, 377–399.
- Gibson, L.J., Ashby, M.F., 1997. *Cellular Solids: Structure and Properties*. Cambridge University Press, Cambridge, UK.
- Hutchinson, J.R., Miller, C.E., Fritsch, G., Hildebrandt, T., 2008. The anatomical foundation for multidisciplinary studies of animal limb function: examples from dinosaur and elephant limb imaging studies. In: Frey R., Endo, H. (Eds.), *Digital Imaging and the Transformation of the Anatomical Sciences: Towards a New Morphology*. Springer, Berlin (in press).
- Keenan, M.J., Hegsted, M., Jones, K.L., Delany, J.P., Kime, J.C., Melancon, L.E., Tulley, R.T., Hong, K.D., 1997. Comparison of bone density measurement techniques: DXA and Archimedes’ principle. *Journal of Bone and Mineral Research* 12, 1903–1907.
- Nicholson, P.H.F., Cheng, X.G., Lowet, G., Boonen, S., Davie, M.W.J., Dequeker, J., Van der Perre, G., 1997. Structural and material properties of human vertebral cancellous bone. *Medical Engineering and Physics* 19, 729–737.
- Martens, M., Van Audekercke, R., Delpont, P., De Meester, P., Mulier, J.C., 1983. The mechanical characteristics of cancellous bone at the upper femoral region. *Journal of Biomechanics* 16, 971–983.
- McNamara, L.M., Prendergast, P.J., Schaffler, M.B., 2005. Bone tissue material properties are altered during osteoporosis. *Journal of Musculoskeletal and Neuronal Interactions* 5, 342–343.
- Mitton, D., Rumerhart, C., Hans, D., Meunier, P.J., 1997. The effects of density and test conditions on measured compression and shear strength of cancellous bone from the lumbar vertebrae of ewes. *Medical Engineering and Physics* 19, 464–474.
- Rice, J.C., Cowin, S.C., Bowman, J.A., 1988. On the dependence of the elasticity and strength of cancellous bone on apparent density. *Journal of Biomechanics* 21, 155–168.

- Schaffler, M.B., Burr, D.B., 1988. Stiffness of compact bone: effects of porosity and density. *Journal of Biomechanics* 21, 13–16.
- Schileo, E., Taddei, F., Malandrino, A., Cristofolini, L., Viceconti, M., 2007. Subject-specific finite element models can accurately predict strain levels in long bones. *Journal of Biomechanics* 40, 2982–2989.
- Sharp, D.J., Tanner, K.E., Bonfield, W., 1990. Measurement of the density of trabecular bone. *Journal of Biomechanics* 23, 853–857.
- Wolf, J., 1892. *Das Gesetz der Transformation der Knochen*. Hirschwald, Berlin.
- Zioupos, P., Aspden, R.M., 2000. Density, material quality and quantity issues in OP cancellous bone. In: *Proceedings of the European Society of Biomechanics*, Dublin, Ireland, p. 327.
- Zioupos, P., Cook, R., Aspden, R.M., Coats, A.M., 2008. Bone quality issues and matrix properties in OP cancellous bone. In: Hammer, J., Nerlich, M., Dendorfer, S. (Eds.), *Medicine meets Engineering*. IOS Press, The Netherlands, pp. 238–245.